



Research article



Simulation of a micro-evaporator for a single horizontal 1-mm circular micro-tube

Simulación de un micro-evaporador para un micro-tubo horizontal circular de 1-mm

César Manuel Valencia-Castillo¹ , Giuseppe Zummo² , Luca Saraceno² , Felipe Noh-Pat³ ,
Pedro Cruz-Alcántar⁴ 

¹CARHS, Universidad Autónoma de San Luis Potosí, Carr. Tamazunchale - San Martín Km. 5, 79960 Tamazunchale, San Luis Potosí, México

²Energy Technologies Department, ENEA, Via Anguillarese 301, 00123, Roma, Italia

³Facultad de Ingeniería, Universidad Autónoma de Campeche, Predio s/n Col. ExHacienda Kalá, 24085 Campeche, Campeche, México

⁴COARA, Universidad Autónoma de San Luis Potosí, Carr. Central Km 5+600, 78700 Matehuala, San Luis Potosí, México

Corresponding author: César Manuel Valencia-Castillo, CARHS, Universidad Autónoma de San Luis Potosí, Carr. Tamazunchale - San Martín Km. 5, 79960 Tamazunchale, San Luis Potosí, México. E-mail: cesar.valencia@uaslp.mx. ORCID: [0000-0003-3831-8121](https://orcid.org/0000-0003-3831-8121).

Received: March 31, 2023

Accepted: May 22, 2023

Published: June 6, 2023

Abstract. - *Flow boiling into micro-channels is a good option of cooling solutions for electronic devices. Numerical simulations allow designing correctly before manufacturing. In this paper, the results of a steady-state one-dimensional simulation are presented for a single horizontal circular 1-mm tube. Through the refrigerant flows, two regions are distinguished: subcooled liquid flow and two-phase flow. Typical equations and correlations have been used for subcooled liquid flow; while one theoretical model has been used for two-phase flow. The results presented here are those by using perfluorohexane, which is used in the formulation of FC-72, a refrigerant for cooling electronic devices. For the range of tested parameters, the next conclusions come: i) from the point of view of choosing the pump, the highest subcooled level, and inlet pressure should be preferred; ii) in order to avoid the critical heat flux condition, the lowest inlet pressure should be preferred; iii) there is a contradiction for choosing the right inlet pressure because is opposite for the point of view of pump selection and critical heat flux condition.*

Keywords: Micro-evaporator; Flow boiling; Numerical simulation; Subcooled liquid flow; Two-phase flow.

Resumen. - *El flujo en ebullición dentro de micro-canales es una buena opción para el enfriamiento de dispositivos electrónicos. Las simulaciones numéricas permiten diseñar correctamente antes de la manufactura. En este artículo, los resultados de una simulación uni-dimensional, en estado estacionario, son presentados para un tubo horizontal circular de 1 mm. Mientras el fluido fluye, se distinguen dos regiones: flujo de líquido sub-enfriado y flujo bifásico. Ecuaciones y correlaciones típicas han sido utilizadas para el flujo de líquido sub-enfriado; mientras que un modelo teórico ha sido utilizado para el flujo bifásico. Los resultados aquí presentados son aquellos utilizando perfluorohexano, el cual es utilizado en la formulación del FC-72, un refrigerante para el enfriamiento de dispositivos electrónicos. Para el rango de los parámetros aquí probados, se obtienen las siguientes conclusiones: i) desde el punto de vista de la selección de la bomba, el nivel más alto de sub-enfriamiento y de presión de ingreso serían preferidos; ii) para evitar la condición de flujo de calor crítico, la más baja presión de ingreso sería preferida; iii) hay una contradicción en la selección de la presión de ingreso correcta porque es opuesta desde el punto de vista de la selección de la bomba y de la condición de flujo de calor crítico.*

Palabras clave: Micro-evaporador; Flujo en ebullición; Simulación numérica; Flujo de líquido sub-enfriado; Flujo bifásico.



1. Introduction

In micro devices, flow boiling into micro-channels seems to be one of the most efficient cooling solutions for high-power density electronic devices, being the main challenge the space limitation.

Research on this topic has been treated theoretically, numerically, and experimentally; Szczukiewicz et al. [1] have published a complete review. Despite the important research accomplishments that have been obtained over the last years, some aspects, including local physical mechanisms related to heat transfer, remain unclear [2].

Generally, numerical simulations provide an efficient tool to estimate the thermodynamic behavior dependent on geometry and operation conditions.

Numerical simulations of flow boiling have been performed in the past years [3-8]. Guo et al. [9] have published a complete review. Despite simulations needing to be compared with experimental results, they serve as a guide to design loops for cooling systems.

The work here presented is the beginning of a project that pretends to simulate for designing of micro-scale cooling systems. Part of the research team is working on the experimental activity. The project's aim is to have a tool to design these systems before manufacturing.

In the present paper, the results of simulations for an evaporator are showed. The evaporator consists of a single 1-mm horizontal circular tube that receives constant heat flux. Inside the tube, fluid is forced to flow. By input physical geometry parameters and fluid properties, among them the outlet quality, the simulation computes the mass flux and the critical heat flux among others outputs.

1.1. Background (Theoretical framework, state of the art)

Cheng & Thome [10] have performed some simulations for flow boiling heat transfer and two-phase pressure drops in microscale channels using R236fa and CO₂ as working fluids. Imke [11] developed a numerical tool to simulate micro-channel flow and heat transfer in compact heat exchangers. Ghajar & Darabi [12] have performed numerical simulations for a micro-loop heat pipe under steady-state conditions, obtaining the optimized geometry dimensions. Magnini & Matar [13] have optimized the design of micro-evaporators via numerical simulations. Cheng et al. [14] have reviewed CO₂ flow boiling heat transfer, flow patterns and two-phase pressure drops in macro- and micro-channel evaporators. Marcinichen & Thome [15] have simulated a two-phase cooling cycle, integrated by a multi micro-channels evaporator. Yildiz [16] has modeled a vapor compression refrigeration cycle for a micro-scale refrigerator.

Karayiannis & Mahmoud [17] have compared the different integrated systems using micro-channels. Oudah et al. [18] have numerically simulated flow boiling R134a refrigerant's heat transfer in a tube having 4.35 mm internal diameter; they claimed an enhancement in the local heat transfer coefficient when the temperature of saturation increased from -7 to -3°C . Lorenzini & Joshi [19] have validated a proposed CFD and heat transfer model for the dielectric refrigerant HFE-7200 under flow boiling conditions, providing evidence that such modeling technique is capable to predict the non-trivial features of two-phase flow in complex cooling layers. Keepaiboon et al. [20] have established the functional relationship of two-phase flow boiling heat transfer correlation of the refrigerant R134a during flow boiling in a rectangular microchannel (at high mass flux) with the Reynolds number, the boiling number,



and the Weber number. Jain et al. [21] have proposed a one-dimensional semi-mechanistic model, combining pressure and heat transfer coefficient, for flow boiling in a rectangular mini/micro-channel, evaluating the transient local heat transfer coefficient in conjunction with the local transient pressure.

Yuan et al. [22] have performed a steady simulation model based on one-dimensional flow direction of flow boiling in micro-channel for refrigerants R134a and R1234ze(E), being to highlight that the local heat transfer coefficient: i) of R1234ze(E) is lower than that of R134a, and ii) decreases (in the two-phase region) along the flow direction, which indicates that the nuclear boiling is dominant. Majumdar et al. [23] have simulated, by solving mass, momentum and energy conservation equations, a configuration of fluid flowing in a vertical heated tube for water and for liquid nitrogen, comparing the experimental data with numerical predictions based on four different correlations, finding that, for the case of boiling water, the predictions using the correlations agreed with the experimental results, while there are large discrepancies for the case of boiling hydrogen. Son & Park [24], by introducing a new numerical phase-change model that reflects the thermal-fluidic discontinuities through the phase interface more faithfully, claimed that their model exhibits superior consistency with the empirical correlation than the Lee model.

Wang & Wu [25] have proposed a novel battery thermal management system (BTMS) using the dielectric, non-flammable HFE-7000 refrigerant, improving the thermal performance of the battery module, showing good agreement between the numerical results and experimental data. Zhou et al. [26] have conducted a one-dimensional numerical study for the heat leak simulation, validating by the experimental data of the loop heat pipe, and showing that their model improves the prediction accuracy for radial heat leak. Bard

et al. [27], by using a number of data science methods and techniques to accurately predict the heat transfer coefficient during flow boiling in mini/micro-channels, have proved that machine learning is an extremely useful tool when predicting the heat transfer coefficient across a variety of different fluids. Moradkhani et al. [28] developed a general explicit model for estimating the saturated flow boiling frictional pressure drop in macro and mini/micro channels heat exchangers, predicting the database with a reasonable value of average absolute relative deviation of 21.34%. Dai et al. [29] have numerically simulated, by the volume of flow (VOF) multiphase model, the flow boiling heat transfer process in a horizontal smooth copper tube, showing that the heat transfer coefficients of simulation have great accuracy with a numerical deviation of $\pm 20\%$.

For modelling of boiling in small channels there are a considerable number of heat transfer correlations. According to Sardeshpande & Ranade [30], one of the major difficulties in modelling two-phase flow is the determination of the geometry of the flow pattern. Kattan et al. [31] argue that the models based on distinguish between flow regimes should be seriously considered for general use. So, it seems that the flow pattern has a crucial role on heat transfer coefficient.

2. Methodology

The simulations have been performed for a smooth horizontal circular tube of inner diameter D and heated length L . A boundary condition of the second kind (Neumann condition), i.e., constant heat flux, has been imposed on the inner surface of the tube. The simulations are performed for steady state, one-dimensional (axial) conditions, using the differential axial distance dz . The working fluid is perfluorohexane (C_6F_{14}), a fluorocarbon that, due to its $T_{sat}(1 atm) = 56.9^\circ C$, is used in



formulation of the FC72, a refrigerant for electronics cooling. Other properties of the perfluorohexane are, at 1 atm: $i_{LV} = 83,559.7 J \cdot kg^{-1}$, $\rho(20^\circ C) = 1,703.4 kg \cdot m^{-3}$, $\mu(20^\circ C) = 0.7229 cP$, $c_p(20^\circ C) = 1,037.5 J \cdot kg^{-1} \cdot K^{-1}$. The fluid enters to the tube at the pressure p_{in} and the subcooled level of ΔT_{sub} (temperature difference below the

saturation temperature as function of p_{in}). The outlet quality x_{out} is an algorithm input as well. The output of the algorithm is the mass flux G required for the input parameters, and the critical heat flux CHF .

Figure 1 outlines the system under analysis.

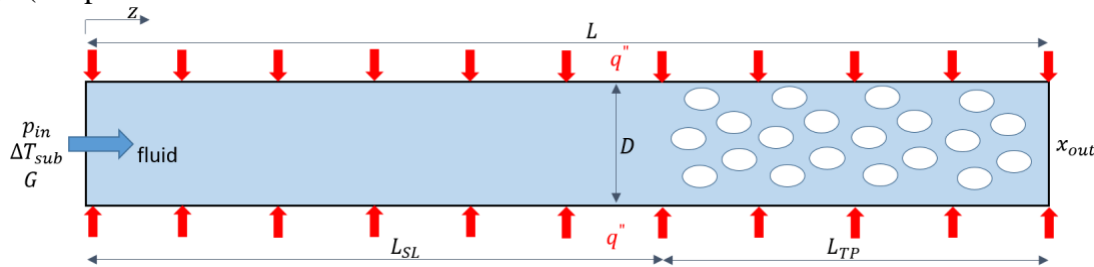


Figure 1. Schematic of the system.

The fixed input parameters are:

$$D = 1 \text{ mm}, L = 100 \text{ mm}, q'' = 100 \text{ kW} \cdot \text{m}^{-2}, x_{out} = 0.3, dz = 0.1 \text{ mm}.$$

While the input parameters that have been tested according to the matrix showed in table 1.

Table 1. Matrix of tested parameters.

| p_{in} [bar] | ΔT_{sub} [K] | | | | |
|----------------|----------------------|---|----|----|----|
| | 0 | 5 | 10 | 15 | 20 |
| 0.5 | ✓ | ✓ | ✓ | ✓ | ✓ |
| 1.0 | ✓ | ✓ | ✓ | ✓ | ✓ |
| 1.4 | ✓ | ✓ | ✓ | ✓ | ✓ |

Figure 2 shows the flow chart of the used algorithm to simulate both, subcooled liquid flow and two-phase flow. During design of an evaporator, it is important to establish the desired flow pattern during two-phase flow, which is related to the quality. It is the reason to consider the outlet quality (x_{out}) as an input parameter.

In this paper, a value of 0.3 has been used as fixed outlet quality, which could resemble, depending on many variables, an up limit of slug to annular flow. Others quantities for this variable should be analyzed for different

applications. The mass flux, needed to maintain the input parameters, is the output of the algorithm. The algorithm has been written in Python. The fluid properties have been obtained using Refprop (version 9.1). All the properties are obtained as function of pressure and temperature.

The classification of the tube scale has been done in the next basis. For the subcooled liquid region, according to Kandlikar et al. [32] a minichannel is a channel whose hydraulic diameter is ranged $3 \text{ mm} \geq D \geq 200 \mu\text{m}$. So, according with this classification, the here analyzed tube is a mini-tube.

For the two-phase region, according to Kew & Cornwell [33], confinement effects are significant for channels having hydraulic diameters such that the confinement number is higher than 0.5, being the confinement number defined as $Co = D^{-1} \{ \sigma / [g(\rho_L - \rho_V)] \}^{0.5}$. For the conditions at the tube outlet, the confinement number of the 15 sets of parameters here analyzed results 0.6992 as minimum and 0.8100 as maximum. So, according to this argument, the here analyzed tube is a micro-tube.



2.1. Subcooled liquid region

For the present analysis, the subcooling level must be $\Delta T_{sub} \geq 0 \text{ K}$.

For $\Delta T_{sub} = 0 \text{ K}$, the conditions in the inlet are those of saturated liquid, so there is not subcooled liquid region ($L_{SL} = 0 \text{ mm}$).

For $\Delta T_{sub} > 0 \text{ K}$, the conditions in the inlet are those of subcooled liquid. In this case, as shown in the flow chart (see figure 2), the convergence is reached when $T_{sat}(p_z) \rightarrow T_z$, where $T_{sat}(p_z)$ is the saturation temperature as function of the local pressure and T_z is the local liquid temperature.

The aforementioned convergence means that the fluid just got the state of saturated liquid at the axial position z . This position represents the axial length from the tube inlet L_{SL} , i.e., the region where the fluid is as subcooled liquid.

Frictional pressure drop has been estimated, for developing laminar region, according to the equation 2 described by Shah & London [34] (based in the work of Hornbeck [35]).

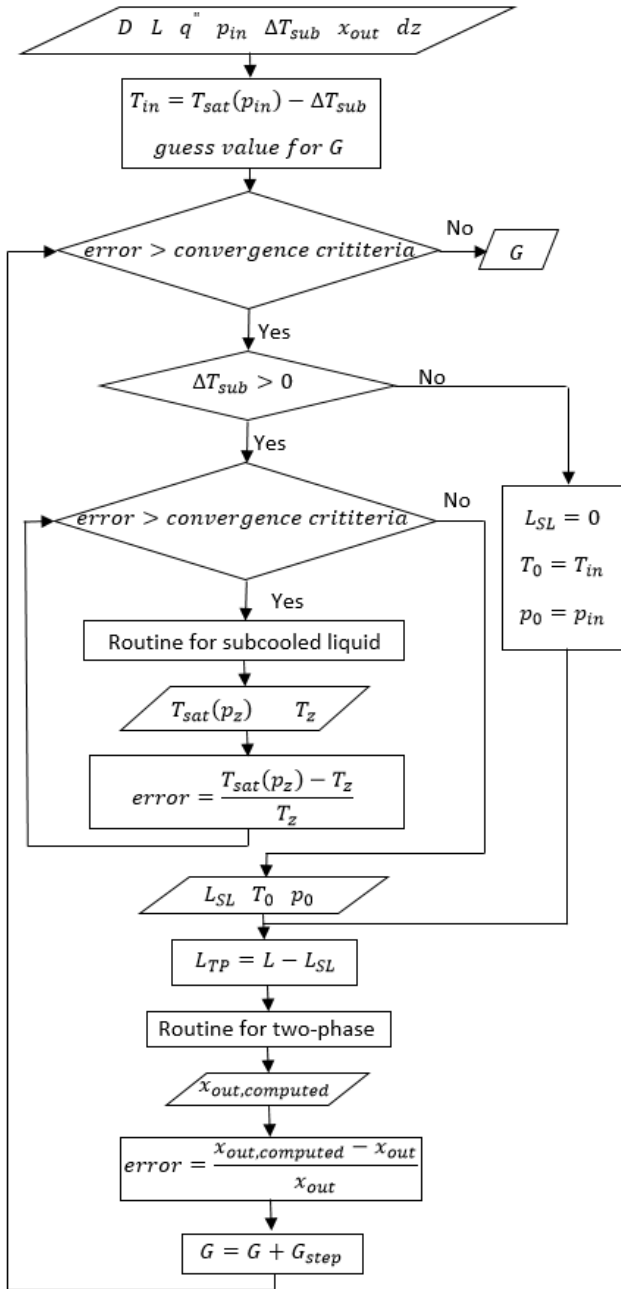


Figure 2. Flow chart of the present algorithm.

$$\frac{dp_f}{dz} = \frac{(1/2)\rho u^2}{dz} \left[13.74(x^+)^{1/2} + \frac{1.25 + 64x^+ - 13.74(x^+)^{1/2}}{1 + 0.00021(x^+)^{-2}} \right] \quad (1)$$

Where $x^+ = (dz/D)/Re$. The length of the hydrodynamic developing region L_h has been estimated by $L_h = 0.05DRe$.

For fully-developed laminar region and turbulent region, frictional pressure drop has been estimated according to:



$$\frac{dp_f}{dz} = \frac{2f\rho u^2}{D} \quad (2)$$

Where f is the Fanning friction factor, being $f = 16/Re$ for fully-developed laminar region, and $f = 0.0791Re^{-0.25}$ for turbulent region, according to the Blasius equation.

So, for the present analysis, if $L_{SL} \leq L_h$ all the subcooled liquid region would be hydrodynamic developing, and if $L_{SL} > L_h$ part the subcooled liquid region would be hydrodynamic developing and the rest would be fully-developed.

Just to point out, gravitational effect has not been taken in account due to the fact that the tube is horizontally oriented.

From an energy balance, temperature has been computed according to:

$$\frac{dT}{dz} = \frac{q''}{\dot{m}c_p} \quad (3)$$

2.2. Two-phase region

The routine for two-phase has been performed by using the theoretical model developed by Revellin & Thome [36]. There, a system of five ordinary differential equations is solved for five dependent variables: liquid and vapor velocities and pressures, u_L , u_V , p_L , and p_V , respectively, and radius of the vapor core r , being the independent variable the axial distance z . The five equations are:

$$\frac{d(A_L u_L)}{dz} dz = -\frac{q'' P}{i_{LV} \rho_L} dz \quad (4a)$$

$$\frac{d(A_V u_V)}{dz} dz = \frac{q'' P}{i_{LV} \rho_V} dz \quad (4b)$$

$$\rho_L \frac{d(A_L u_L^2)}{dz} dz = -A_L \frac{dp_L}{dz} dz + A_i |\tau_{LV}| - A_{LW} |\tau_{LW}| \quad (4c)$$

$$\rho_V \frac{d(A_V u_V^2)}{dz} dz \quad (4d)$$

$$= -A_V \frac{dp_V}{dz} dz + A_i |\tau_{VL}|$$

$$\frac{dp_V}{dz} - \frac{dp_L}{dz} = \frac{d}{dz} \left(\frac{\sigma}{r} \right) \quad (4e)$$

Equations 4a and 4b have been derived by the conservation of mass. Equations 4c and 4d come from conservation of momentum. Finally, equation 4e is the Laplace-Young equation.

The system has been numerically solved using the 4th-order Runge-Kutta method imposing five boundary conditions for $x = 0$ (saturated liquid), i.e. where two-phase region begins. When the tube outlet is reached ($z = L$), an outlet quality is computed.

As shown in the flow chart (see figure 2), the convergence is reached when $x_{out,computed} \rightarrow x_{out}$. The output of the algorithm is the required mass flux for the input parameters.

Once the mass flux has been computed, the entire algorithm runs again to get the critical heat flux. The convergence is reached when a minimal liquid film thickness occurs in the tube outlet, i.e. dry-out condition, according to:

$$\delta = C \frac{D}{2} \left(\frac{u_V}{u_L} \right)^j \left(\frac{(\rho_L - \rho_V)g(D/2)^2}{\sigma} \right)^k \quad (5)$$

Where $C = 0.15$, $j = -3/7$, and $k = -1/7$, according to Revellin & Thome [36].

3. Results and discussions

The figures in this section show results as function of the subcooled level. The results here presented are the contribution in the study of flow boiling inside micro-tube, according with the parametric analysis of table 1.



Verification of the present algorithm has been performed by solving the case presented by Revellin & Thome [36].

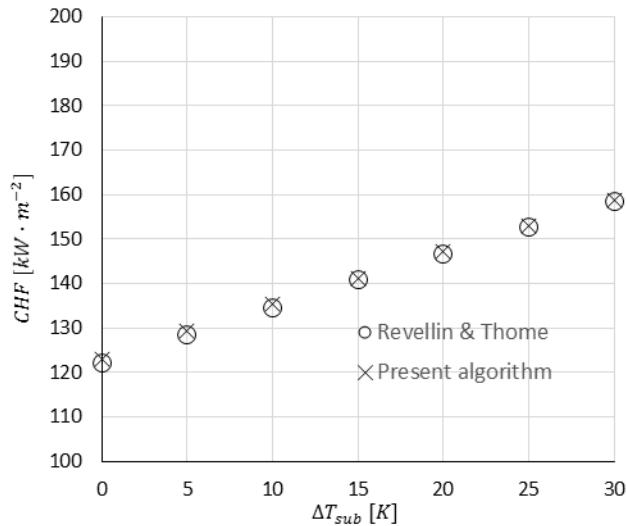


Figure 3. Verification with the results from Revellin & Thome [36].

Figure 3 shows the comparison between the results of Revellin & Thome [36] and the results from the present algorithm. The maximum deviation has been 0.7%, for $\Delta T_{sub} = 0 K$. This small difference could be attributed to the used properties, the used equations in the subcooled liquid, among others. Due to the very small difference, it is having been verified.

Once it has been verified, some simulations have been run. Three inlet pressures are shown in the figures. Note that the value of $\Delta T_{sub} = 0 K$ corresponds to the case when saturated liquid enters to the tube; while $\Delta T_{sub} > 0 K$ to the case when subcooled liquid enters to the tube (the higher ΔT_{sub} , the lower the inlet temperature). The mass flux, together with the pressure drop, are important parameters to select the right pump of the loop.

The *CHF* is an important parameter to design because this condition is always avoided.

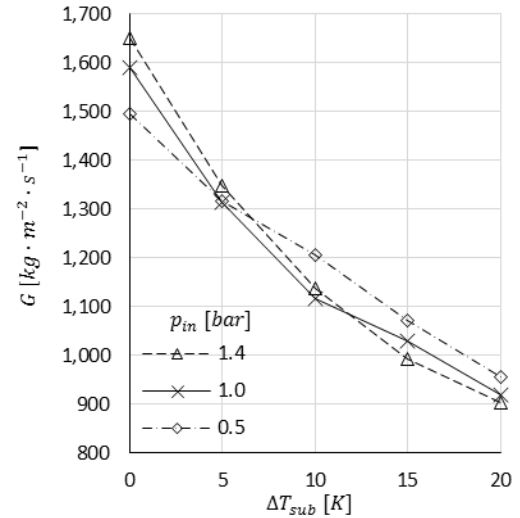


Figure 4. Mass flux as function of subcooled level.

Figure 4 shows the required mass flux according to the subcooled level and the inlet pressure.

As expected, for higher subcooled level, less mass flux is required. For subcooled liquid entering to the tube, less mass flux is required for lower liquid temperature due to it can carry more energy (heat flux) along the tube.

There is not a regular tendency by inlet pressure comparison. For the case when saturated liquid enters to the tube ($\Delta T_{sub} = 0 K$), the highest inlet pressure (1.4 bar) requires more mass flux than the lowest inlet pressure (0.5 bar); while for the highest subcooled level ($\Delta T_{sub} = 20 K$), it is totally opposite.

From the point of view of the mass flux, in order to reduce the pump power, higher subcooled level should be chosen.

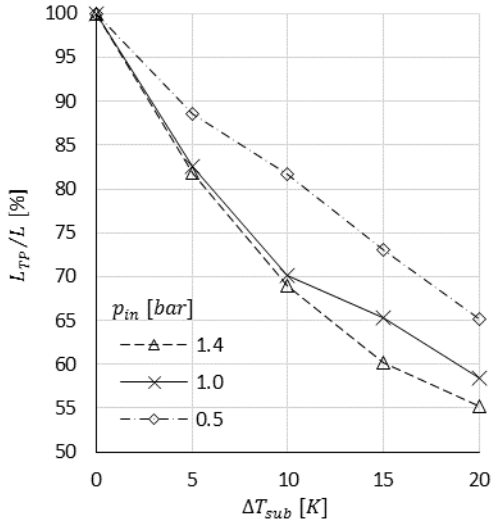


Figure 5. Ratio of length of two-phase and total length as function of subcooled level.

Figure 5 shows the ratio of length of two-phase and the total heated length according to the subcooled level and the inlet pressure.

For the case when saturated liquid enters to the tube ($\Delta T_{sub} = 0$ K), the entire tube is in two-phase flow ($L_{TP}/L = 100\%$). As subcooled level increases, the length of two-phase decreases because the fluid needs more length of subcooled liquid in order to reach the state of saturated liquid.

For higher inlet pressure, less length of two-phase exists. It seems that fluid properties for higher inlet pressure leads to need longer length of subcooled liquid in order to get the state of saturated liquid.

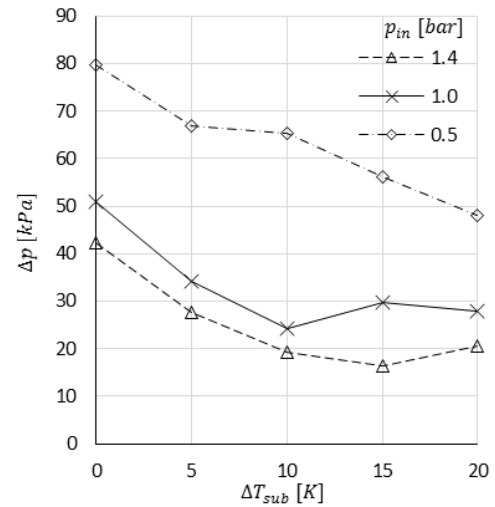


Figure 6. Pressure drop as function of subcooled level.

Figure 6 shows the pressure drop along the tube according to the subcooled level and the inlet pressure. It is possible to see a slight tendency to reduce the pressure drop for higher subcooled levels.

As high the inlet pressure as less pressure drop. It is because the fluid has more enthalpy for higher pressure. From the point of view of the pressure drop, in order to reduce the pump power, higher inlet pressure should be chosen. Note that this pressure drop is only of the evaporator. In order to choose a pump, it is necessary to analyze all the loop components.

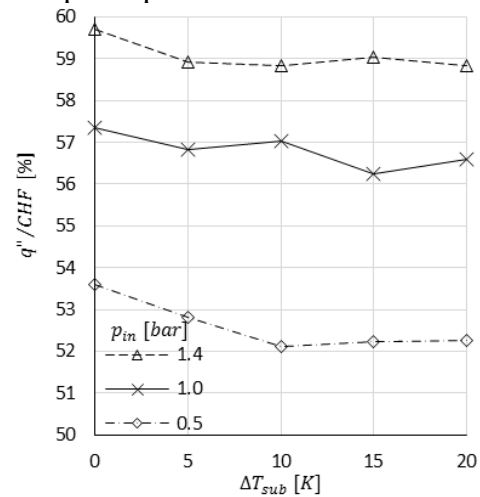


Figure 7. Ratio of heat flux and CHF as function of subcooled level.



Figure 7 shows the ratio of the actual heat flux and the critical heat flux according to the subcooled level and the inlet pressure. It is a very slight reduction of this ratio for higher subcooled levels, for higher inlet pressure, the actual heat flux is closer to the CHF; for example, for $p_{in} = 1.4 \text{ bar}$ the actual heat flux represents around 59% of the CHF, while for $p_{in} = 0.5 \text{ bar}$ represents around 53%.

From the point of view of the CHF, it would be preferred the lowest inlet pressure in order to be farther of this condition. Finally, note that the decision of the inlet pressure is a quandary because it should be the highest thinking in the pump selection but the lowest thinking in the critical heat flux.

5. Conclusions

From the simulations for an evaporator showed in this paper, the next conclusions are found.

- To choose the right pump, the highest subcooled level and inlet pressures should be preferred.
- To avoid the critical heat flux condition, the lowest inlet pressure should be preferred.
- The right inlet pressure is difficult to decide because is opposite for the point of view of pump selection and critical heat flux condition.
- The results here presented are for a circular tube. The next step will be to simulate for a rectangular channel.

6. Acknowledgment

The authors thank to the PRODEP, granted by the Ministry of Education of Mexico.

7. Authorship acknowledgment

César Manuel Valencia-Castillo: Methodology; Analysis; Resources; Documentary research; Original draft; Script. Giuseppe Zummo: Ideas; Analysis; Resources. Luca Saraceno: Ideas; Analysis. Felipe Noh-

Pat: Methodology; Analysis; Documentary research; Script. Pedro Cruz-Alcántar: Script; Edition.

Nomenclature

| Symbol | Description | SI unit |
|-------------------|--|--------------------------------|
| Roman | | |
| A | Cross sectional area | m^2 |
| c_p | Specific heat capacity | $J \cdot kg^{-1} \cdot K^{-1}$ |
| CHF | Critical heat flux | $W \cdot m^{-2}$ |
| dz | Differential axial length | m |
| D | Inner tube diameter | m |
| f | Fanning friction factor | – |
| g | Gravitational acceleration | $m \cdot s^{-2}$ |
| G | Mass flux | $kg \cdot m^{-2} \cdot s^{-1}$ |
| i | Specific enthalpy | $J \cdot kg^{-1}$ |
| L | Axial heated length | m |
| \dot{m} | Mass flow rate | $kg \cdot s^{-1}$ |
| p | Pressure | Pa |
| P | Inner tube perimeter | m |
| q'' | Heat flux | $W \cdot m^{-2}$ |
| r | Radius of the vapor core | m |
| Re | Reynolds number | – |
| T | Temperature | $^{\circ}C$ |
| u | Velocity | $m \cdot s^{-1}$ |
| x | Mass quality | – |
| x^+ | Dimensionless length | – |
| z | Axial distance from the inlet | m |
| Greek | | |
| δ | Liquid film thickness | m |
| Δp | Pressure drops | Pa |
| ΔT | Temperature difference | K |
| μ | Dynamic viscosity | $Pa \cdot s$ |
| ρ | Density | $kg \cdot m^{-3}$ |
| σ | Surface tension | $N \cdot m^{-1}$ |
| τ | Shear stress | $N \cdot m^{-2}$ |
| Subscripts | | |
| f | Frictional | |
| i | Liquid-Vapor interfacial | |
| in | Tube inlet | |
| L | Liquid phase | |
| LV | Change of phase (when i) or Liquid-Vapor (when τ) | |
| LW | Liquid-Wall | |
| out | Tube outlet | |
| sat | Saturated | |
| SL | Subcooled liquid | |
| sub | Subcooling | |
| TP | Two-phase | |
| V | Vapor phase | |
| z | Axial local position | |
| 0 | Indicative for saturated liquid | |



References

- [1] S. Szczukiewicz, M. Magnini, and J. R. Thome, "Proposed models, ongoing experiments, and latest numerical simulations of microchannel two-phase flow boiling," *Int. J. Multiph. Flow*, vol. 59, pp. 84-101, 2014. <https://doi.org/10.1016/j.ijmultiphaseflow.2013.10.014>
- [2] C. B. Tibiriçá and G. Ribatski, "Flow boiling in micro-scale channels - Synthesized literature review," *Int. J. Refrig.*, vol. 36, no. 2, pp. 301-324, 2013. <https://doi.org/10.1016/j.ijrefrig.2012.11.019>
- [3] A. Mukherjee and S. G. Kandlikar, "Numerical simulation of growth of a vapor bubble during flow boiling of water in a microchannel," *Microfluid. Nanofluid.*, vol. 1, pp. 137-145, 2005. <https://doi.org/10.1007/s10404-004-0021-8>
- [4] R. Zhuan and W. Wang, "Simulation of subcooled flow boiling in a micro-channel," *Int. J. Refrig.*, vol. 34, no. 3, pp. 781-795, 2011. <https://doi.org/10.1016/j.ijrefrig.2010.12.004>
- [5] R. Zhuan and W. Wang, "Flow pattern of boiling in micro-channel by numerical simulation," *Int. J. Heat Mass Transfer*, vol. 55, no. 5-6, pp. 1741-1753, 2012. <https://doi.org/10.1016/j.ijheatmasstransfer.2011.11.029>
- [6] M. Magnini, B. Pulvirenti, and J. R. Thome, "Numerical investigation of hydrodynamics and heat transfer of elongated bubbles during flow boiling in a microchannel," *Int. J. Heat Mass Transfer*, vol. 59, pp. 451-471, 2013. <https://doi.org/10.1016/j.ijheatmasstransfer.2012.12.010>
- [7] M. Magnini, B. Pulvirenti, and J. R. Thome, "Numerical investigation of the influence of leading and sequential bubbles on slug flow boiling within a microchannel," *Int. J. Therm. Sci.*, vol. 71, pp. 36-52, 2013. <https://doi.org/10.1016/j.ijthermalsci.2013.04.018>
- [8] M. Magnini and J. R. Thome, "Computational study of saturated flow boiling within a microchannel in the slug flow regime," *ASME J. Heat Transfer*, vol. 138, no. 2, pp. 021502, 2016. <https://doi.org/10.1115/1.4031234>
- [9] Z. Guo, D. F. Feltcher, and B. S. Haynes, "A review of computational modelling of flow boiling in microchannels," *J. Comput. Multiphase Flows*, vol. 6, no. 2, pp. 79-110, 2014. <https://doi.org/10.1260/1757-482X.6.2.79>
- [10] L. Cheng and J. R. Thome, "Cooling of microprocessors using flow boiling of CO₂ in a micro-evaporator: Preliminary analysis and performance comparison," *Appl. Therm. Eng.*, vol. 29, no. 11-12, pp. 2426-2432, 2009. <https://doi.org/10.1016/j.applthermaleng.2008.12.019>
- [11] U. Imke, "Porous media simplified simulation of single- and two-phase flow heat transfer in micro-channel heat exchangers," *Chem. Eng. J.*, vol. 101, no. 1-3, pp. 295-302, 2004. <https://doi.org/10.1016/j.cej.2003.10.012>
- [12] M. Ghajar and J. Darabi, "Numerical modeling of evaporator surface temperature of a micro loop heat pipe at steady-state condition," *J. Micromech. Microeng.*, vol. 15, no. 10, pp. 1963-1971, 2005. <https://doi.org/10.1088/0960-1317/15/10/024>
- [13] M. Magnini and O. K. Matar, "Optimizing the design of micro-evaporators via numerical simulations," presented at the 16th UK Heat Transfer Conference, pp. 163-168, 2021. https://doi.org/10.1007/978-981-33-4765-6_30
- [14] L. Cheng, G. Xia, and J. R. Thome, "Flow boiling heat transfer and two-phase flow phenomena of CO₂ in macro- and micro-channel evaporators: Fundamentals, applications and engineering design," *Appl. Therm. Eng.*, vol. 195, pp. 117070, 2021. <https://doi.org/10.1016/j.applthermaleng.2021.117070>
- [15] J. B. Marcinichen and J. R. Thome, "New novel green computer two-phase cooling cycle: A model for its steady-state simulation," in *Proc. of the 23rd Int. Conf. on Efficiency, Cost, Optimization, Simulation and Environmental Impact of Energy Systems-ECOS2010*, Lausanne, Switzerland 2010.



- [16] S. Yildiz, "Design and simulation of a vapor compression refrigeration cycle for a micro refrigerator," M.S. thesis. Graduate School of Natural and Appl. Sci. of Middle East Tech. Univ., 2010. [Online]. Available: <https://etd.lib.metu.edu.tr/upload/12612133/index.pdf>
- [17] T. G. Karayiannis and M. M. Mahmoud, "Flow boiling in microchannels: Fundamentals and applications," *Appl. Therm. Eng.*, vol. 115, pp. 1372-1397, 2017. <https://doi.org/10.1016/j.applthermaleng.2016.08.063>
- [18] M. H. Oudah, M. K. Mejbil, and M. K. Allawi, "R134a flow boiling heat transfer (FBHT) characteristics in a refrigeration system," *J. Mech. Eng. Res. Dev.*, vol. 44, no. 4, pp. 69-83, 2021.
- [19] D. Lorenzini and Y. Joshi, "Numerical modeling and experimental validation of two-phase microfluidic cooling in silicon devices for vertical integration of microelectronics," *Int. J. Heat Mass Transfer*, vol. 138, pp. 194-207, 2019. <https://doi.org/10.1016/j.ijheatmasstransfer.2019.04.036>
- [20] C. Keepaiboon, A.S. Dalkilic, O. Mahian, H.S. Ahn, S. Wongwises, P.K. Mondal, and M.S. Shadloo, "Two-phase flow boiling in a microfluidic channel at high mass flux," *Phys. Fluids*, vol. 32, no. 9, 093309, 2020. <https://doi.org/10.1063/5.0023758>
- [21] S. Jain, P. Jayaramu, and S. Gedupudi, "Modeling of pressure drop and heat transfer for flow boiling in a mini/micro-channel of rectangular cross-section," *Int. J. Heat Mass Transfer*, vol. 140, pp. 1029-1054, 2019. <https://doi.org/10.1016/j.ijheatmasstransfer.2019.05.089>
- [22] X. Yuan, P. Zhao, J. Huang, J. Wu, D. Zhou, R. Wang, J. Hu, and B. Qu, "Simulation research on flow boiling and heat transfer of micro-channel for electronic cooling," *J. Phys. Conf. Ser.*, vol. 2224, 2021. <https://doi.org/10.1088/1742-6596/2224/1/012052>
- [23] Majumdar, C. Ursachi, A. LeClair, and J. Hartwig, "Numerical modeling of boiling in a heated tube," presented at the Space Cryogenic Workshop, Southbury, CT, 2019.
- [24] J.H. Son and I.S. Park, "Numerical simulation of phase-change heat transfer problems using heat fluxes on phase interface reconstructed by contour-based reconstruction algorithm," *Int. J. Heat Mass Transfer*, vol. 156, 119894, 2020. <https://doi.org/10.1016/j.ijheatmasstransfer.2020.119894>
- [25] Y.F. Wang and J.T. Wu, "Thermal performance predictions for an HFE-7000 direct flow boiling cooled battery thermal management system for electric vehicles," *Energy Convers. Manage.*, vol. 207, 112569, 2020. <https://doi.org/10.1016/j.enconman.2020.112569>
- [26] L. Zhou, Z. G. Qu, G. Chen, J. Y. Huang, and J. Y. Miao, "One-dimensional numerical study for loop heat pipe with two-phase heat leak model," *Int. J. Therm. Sci.*, vol. 137, pp. 467-481, 2019. <https://doi.org/10.1016/j.ijthermalsci.2018.12.019>
- [27] A. Bard, Y. Qiu, C. R. Kharangate, and R. French, "Consolidated modeling and prediction of heat transfer coefficients for saturated flow boiling in mini/micro-channels using machine learning methods," *Appl. Therm. Eng.*, vol. 210, 118305, 2022. <https://doi.org/10.1016/j.applthermaleng.2022.118305>
- [28] M. A. Moradkhani, S. H. Hosseini, P. Morshedi, M. Rahimi, and S. Mengjie, "Saturated flow boiling inside conventional and mini/micro channels: A new general model for frictional pressure drop using genetic programming," *Int. J. Refrig.*, vol. 132, pp. 197-212, 2021. <https://doi.org/10.1016/j.ijrefrig.2021.09.022>
- [29] Y. Dai, N. Zhang, S. Tian, and H. Du, "Numerical study of flow boiling heat transfer of propane in a horizontal smooth copper tube," *Heat Transfer Res.*, vol. 51, no. 18, pp. 1653-1667, 2020.



<https://doi.org/10.1615/HeatTransRes.2020034503>

[30] M. V. Sardeshpande and V. V. Ranade, “Two-phase flow boiling in small channels: A brief review,” *Sadhana*, vol. 38, pp. 1083-1126, 2013. <https://doi.org/10.1007/s12046-013-0192-7>

[31] N. Kattan, J. R. Thome, and D. Favrat, “Flow boiling in horizontal tubes: Part 1-Development of a diabatic two-phase flow pattern map,” *ASME J. Heat Transfer*, vol. 120, no. 1, pp. 140-147, 1998. <https://doi.org/10.1115/1.2830037>

[32] S. Kandlikar, S. Garimella, D. Li, S. Colin, and M. R. King, *Heat transfer and fluid flow in minichannels and microchannels*. Kidlington, Oxford, UK: Elsevier Ltd, 2006.

[33] P. A. Kew and K. Cornwell, “Correlations for the prediction of boiling heat transfer in small-diameter channels,” *Appl. Therm. Eng.*, vol. 17, no. 8-10, pp. 705-715, 1997. [https://doi.org/10.1016/S1359-4311\(96\)00071-3](https://doi.org/10.1016/S1359-4311(96)00071-3)

[34] R. K. Shah and A. L. London, *Laminar flow forced convection in ducts*. New York: Elsevier Inc., 1978.

[35] R. W. Hornbeck, “Laminar flow in the entrance region of a pipe,” *Appl. Sci. Res.*, vol. 13, pp. 224-232, 1964. <https://doi.org/10.1007/BF00382049>

[36] R. Revellin and J. R. Thome, “A theoretical model for the prediction of the critical heat flux in heated microchannels,” *Int. J. Heat Mass Transfer*, vol. 51, no. 5-6, pp. 1216-1225, 2008. <https://doi.org/10.1016/j.ijheatmasstransfer.2007.03.002>.

Derechos de Autor (c) 2023 César Manuel Valencia-Castillo, Giuseppe Zummo, Luca Saraceno, Felipe Noh-Pat, Pedro Cruz-Alcántar



Este texto está protegido por una licencia [Creative Commons 4.0](https://creativecommons.org/licenses/by/4.0/).

Usted es libre para compartir —copiar y redistribuir el material en cualquier medio o formato— y adaptar el documento —remezclar, transformar y crear a partir del material— para cualquier propósito, incluso para fines comerciales, siempre que cumpla la condición de:

Atribución: Usted debe dar crédito a la obra original de manera adecuada, proporcionar un enlace a la licencia, e indicar si se han realizado cambios. Puede hacerlo en cualquier forma razonable, pero no de forma tal que sugiera que tiene el apoyo del licenciante o lo recibe por el uso que hace de la obra.

[Resumen de licencia](#) - [Texto completo de la licencia](#)